

## REVIEW

[View Article Online](#)  
[View Journal](#) | [View Issue](#)


Cite this: RSC Adv., 2018, 8, 33551

## Oxygen vacancies of the $\text{TiO}_2$ nano-based composite photocatalysts in visible light responsive photocatalysis

Buanya Beryl Adormaa,<sup>†</sup> Williams Kweku Darkwah  <sup>†\*</sup> and Yanhui Ao  \*

The  $\text{TiO}_2$  nano-based composite photocatalyst is best known for application in solving the recent issues related to energy and environmental purification. Due to the low cost, nontoxicity, chemical stability and high efficiency of  $\text{TiO}_2$ , it is unquestionably one of the most considered materials in environmental treatment. In this systematic review, we reveal the outstanding potential of oxygen vacancy in photocatalysis, and discuss the contemporary advancement in the photocatalytic activities, productivity, preparation methods and oxygen vacancy of the  $\text{TiO}_2$  nano-based composite photocatalyst for environmental treatment and energy as well as wastewater treatment. This exposé is anticipated to enlighten researchers and engineers on the specific management and assessment of the environment, which warrants prospective research into developing appropriate mechanisms for energy, wastewater treatment and environmental purification.

Received 14th June 2018

Accepted 17th August 2018

DOI: 10.1039/c8ra05117h

[rsc.li/rsc-advances](http://rsc.li/rsc-advances)

### 1. Introduction

Currently, research efforts have shifted toward semiconductor photocatalysts such as  $\text{TiO}_2$ ,  $\text{ZnO}$ ,  $\text{g-C}_3\text{N}_4$ , *etc.*, due to the ability of these metals to convert pollutants into  $\text{CO}_2$  and  $\text{H}_2\text{O}$  for environmental applications such as biofuel production and wastewater treatment. For modest and cost-effective treatment, additional efficient photocatalysts are highly preferred to parallel the extensively used  $\text{TiO}_2$ . The field of water

photocatalysis has experienced tremendous growth, following the discovery of photocatalytic  $\text{H}_2$  production in the 1980s and the photocatalysis and hydrophilicity of  $\text{TiO}_2$  films by Honda and Fujishima in the 1990s, and other scientists in the early 70s.<sup>67–72</sup> Further studies have revealed that industrial applications in this area have been wonderfully accomplished since the early 90s based on the outcomes from these basic research efforts.<sup>6,105–107</sup>

Photocatalysis is the speeding up of oxidation and reduction reactions, brought about through the activation of a catalyst consisting of a semiconductor either alone or in combination with metal/organic/organometallic promoters, through light absorption and the subsequent charge and/or energy transfer, which can lead to the transformation of a pollutant. It must be noted that during the photocatalytic reaction, two actions must

Key Laboratory of Integrated Regulation and Resource Development on Shallow Lakes, Ministry of Education, Environmental Engineering Department, College of Environment, Hohai University, Nanjing, China. E-mail: andyao@hhu.edu.cn; wkdarkwah@hhu.edu.cn; williams.darkwah@stu.ucc.edu.gh; Tel: +8613770610843

<sup>†</sup> These authors contributed equally to this work.



Buanya Beryl Adormaa is a Doctoral degree student at the College of Environment, Hohai University, Nanjing, China. She received her M.Sc. degree from Hohai University, Nanjing, China. Her research interest is mainly focused on photocatalysis-based water remediation technology using nanomaterials.



Williams Kweku Darkwah is a Master's degree student in the Environmental Engineering Department, College of Environment, Hohai University, Nanjing, China. He received his B.Sc. from the University of Cape Coast, Ghana. His research interest is mainly focused on photocatalysis-based water remediation technology using nanomaterials.



occur simultaneously in order for the successful production of reactive oxidizing species to occur. Typically, the first involves the oxidation of dissociatively adsorbed  $\text{H}_2\text{O}$  by photogenerated holes, the second involves the reduction of an electron acceptor (typically dissolved oxygen) by photoexcited electrons; these reactions lead to the production of a hydroxyl and superoxide radical anion, respectively.<sup>68,69,97,103,104</sup> In the area of photocatalysis, energy saving green tools are the ultimate, in accordance with photoinduced water cleavage to  $\text{TiO}_2$  electrodes, a phenomenon discovered by the pioneers in the field.<sup>1</sup> It is believed that  $\text{TiO}_2$  photocatalysis is currently one of the best in the recent research in nanoscience and nanotechnology.

There have been many successful reports on the potential applications of  $\text{TiO}_2$  photocatalysts in water and environmental purification and management in the past few decades. In solving the recent issues related to energy and environmental purification, heterogeneous metal oxide semiconductor photocatalysts are best known. Due to the low-cost, nontoxicity, chemical stability and high efficiency of  $\text{TiO}_2$ , it is unquestionably one of the most considered materials by researchers in the field of photocatalysis. However, the low quantum efficiency of  $\text{TiO}_2$  in photocatalytic mechanisms and the ineffective use of visible light for  $\text{H}_2$  harvesting, which mainly comes from its high recombination rate of photogenerated electron–hole pairs and wide band gap, have become problematic in prospective applications.<sup>9,73,74</sup>

Scientists in the field have adopted various approaches for the improvement of the photocatalytic efficacy of  $\text{TiO}_2$ . These strategies can be summarized as morphological modifications, such as increased surface area and porosity, or as chemical modifications, by the incorporation of additional components into the  $\text{TiO}_2$  structure. Three basic strategies have been adopted for the structural modification, namely, doping with metallic/non-metallic elements or co-doping of metallic and non-metallic elements,<sup>9,108–110</sup> modification through the introduction of defects such as oxygen vacancies and  $\text{Ti}^{3+}$  in the band gap,<sup>111,112</sup> and surface modification by treatment techniques.<sup>113–115</sup> Currently, the attention is centered on oxygen vacancies, which occur naturally in oxides, due to the vital role they play in the physical characteristics of materials; oxygen

vacancies may be positive or negative. Oxygen vacancies occur when the number of oxygens in a particular compound is less than what it is supposed to be to make a perfect crystal lattice. This results in materials such as  $\text{ZnFe}_2\text{O}_4$ , where  $\text{ZnO}$  and  $\text{Fe}_2\text{O}_3$  are chosen as starting compounds.

This review is centered on the ability and effectiveness of the prospective applications of oxygen vacancies and photocatalysis using  $\text{TiO}_2$  composites for energy, wastewater and environmental treatment in order to design future implementations to solve environmental problems. This is attractive for ecological uses such as water purification, purified biofuel production and wastewater treatment. Researchers in this field are doing their best in one way or the other to use these composites to solve the environmental crises. This discussion tackles the use of oxygen vacancies of  $\text{TiO}_2$  nano-based composites in photocatalysis to solve environmental concerns such as water treatment and related issues.

## 2. Review

### 2.1. Photocatalysis

Environmental remediation technology such as aromatic oxygen vacancy compounds and  $\text{NO}_x$  have been suggested by scientists in recent years for the treatment of urban pollution; thus leading to the use of photocatalytic self-cleaning and depolluting constituents. The photocatalytic properties of a thin layer of  $\text{TiO}_2$  entrenched in paints or concrete or placed at the surface of the particle influences the choice of these viable products. Photocatalysis is designed to harvest visible light (the major component of solar radiation that reaches the Earth's surface) using photocatalysts to drive chemical transformations (Fig. 1 and 3). The use of  $\text{TiO}_2$  photocatalysts as an evolving pollution control technology has been stated in numerous fields of science.<sup>9,22,31,37,38</sup> It, therefore, seems that the actual influence and efficiency on the quality of water of these novel advancements have not been fully demonstrated to date but it has been revealed in a very restricted way. Photocatalysis embraces a class of reactions that use a catalyst activated by light and the decomposition of organic composites into water and carbon dioxide, leading to the fascinating properties of surfaces covered with a photocatalyst; these can shield against coating by fouling matter, are self-cleaning, antibacterial and viricidal.

Heterogeneous photocatalysis in gas and liquid phase remediation has been intensively described by many researchers. Typically, the complete procedure is made up of five separate steps (Fig. 2): allocation of the reactants in the gas or liquid phase to the surface, adsorption of at least one of the reactants, reaction in the adsorbed phase, desorption of the product(s), and removal of the products from the interface region.

The third step is where the photocatalytic nature of certain metal oxides plays a role despite all the steps usually found in all heterogeneous processes. Semiconductor catalysts such as  $\text{TiO}_2$ ,  $\text{ZnO}$ ,  $\text{ZrO}_2$ ,  $\text{CeO}_2$  etc., with photons carrying energy equal to or in excess of its band gap, create electron–hole pairs similar to photoinduced electron transfer and the absorption of light promotes one electron into the conduction band. The oxide may



*Yanhui Ao, Ph.D., is a Professor at Hohai University, Nanjing, China. He received his Doctorate degree from the Southeast University, Nanjing, China. He has published more than 130 academic papers and also has more than 7 patents. His research interests mainly focus on new photocatalysis-based water remediation technology using nanomaterials, water resources protection, the behaviour of manufactured nanomaterials in the environment, and environmentally friendly materials.*



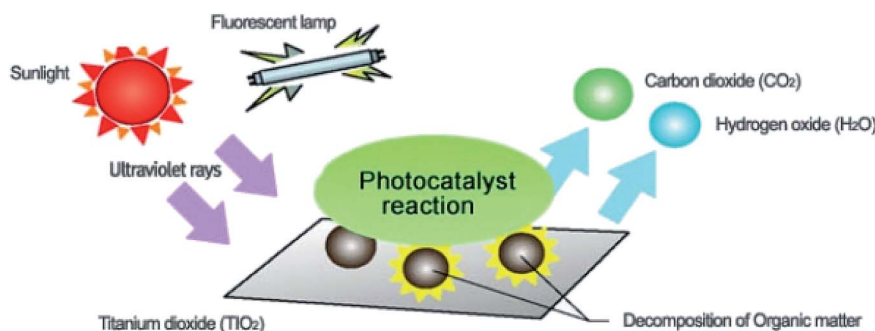


Fig. 1 Schematic diagram demonstrating the photocatalysis mechanism.

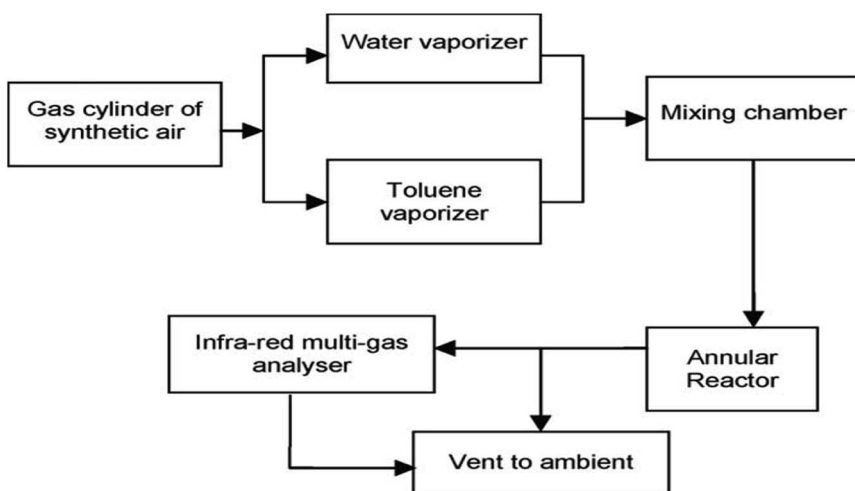


Fig. 2 Flow diagram of the photocatalytic reaction system set-up.

transfer its electron to any adsorbed electron acceptor (thereby promoting its reduction), while the hole (or the electron vacancy) may accept an electron from an adsorbed donor (promoting its oxidation).

$\text{TiO}_2$  photocatalysis happens when the energy of the photons is enough to promote the electrons in the valence band to jump to the conduction band; this occurs in three steps:

(a) Photon absorption and electron–hole pair generation.

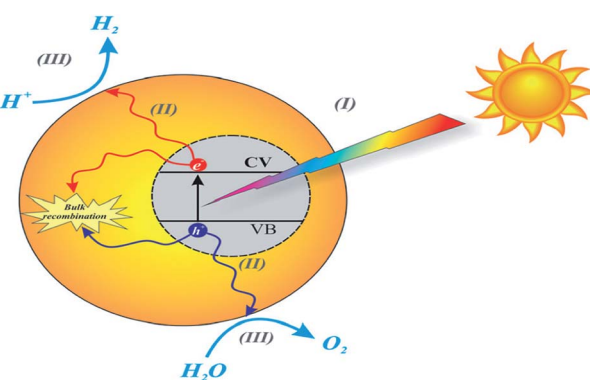


Fig. 3 Schematic diagram of the basic mechanisms of the photocatalytic activity of water splitting. Reproduced with permission.<sup>64</sup> Copyright 2015, *Nanoscale*. The Royal Society of Chemistry.

(b) Charge separation and migration to surface reaction sites or to recombination sites.

(c) Surface chemical reactions at active sites containing donor oxidation at valence-band holes and acceptor reduction at electron centers (Fig. 4).

Numerous defects associated with photocatalytic principles have been identified by researchers. During photocatalysis, cation radicals<sup>17</sup> can be produced by injecting charge from

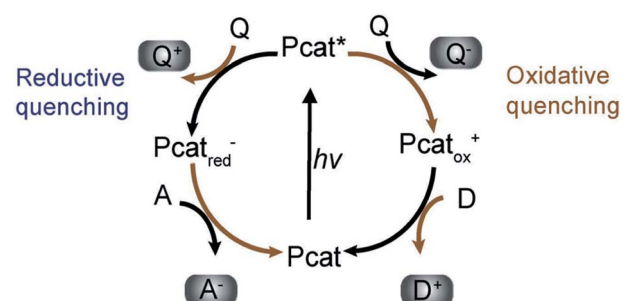


Fig. 4 Photoredox catalysis by the photocatalyst. The oxidation steps are portrayed on the right; the reduction steps are shown on the left. Pcat: photocatalyst, Q: quencher, D: donor, A: acceptor. Reproduced with permission.<sup>62</sup> Copyright 2009, Wiley-VCH Verlag GmbH & Co. KGaA, Weinheim.

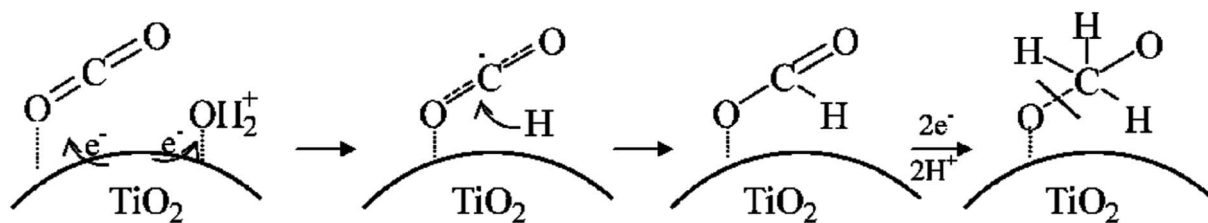


Fig. 5 The mechanism of photoreduction of  $\text{CO}_2$  to the methoxyl radical on  $\text{TiO}_2$  in the presence of water during the photocatalytic reaction. Reproduced with permission.<sup>63</sup> Copyright 2011, American Chemical Society.

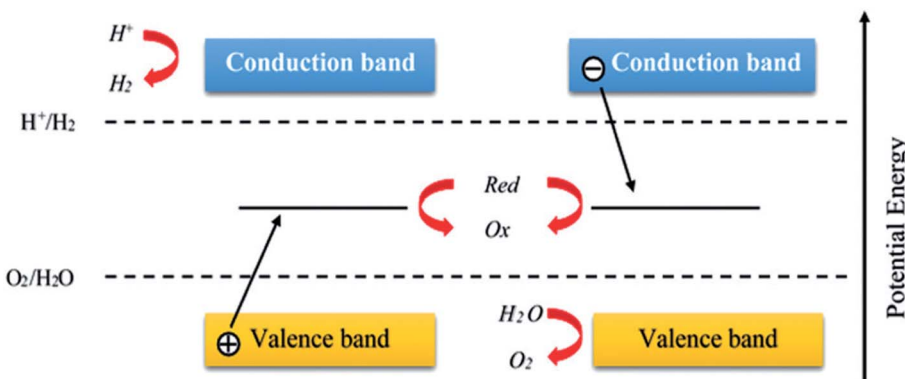


Fig. 6 Schematic diagram showing the general water splitting ability of photocatalysts in the Z-scheme system. Reproduced with permission.<sup>64</sup> Copyright 2015, *Nanoscale*. The Royal Society of Chemistry.

excited molecules into the conduction band of  $\text{TiO}_2$  (Fig. 4 and 5).

Irradiation is usually the starting process in  $\text{TiO}_2$  photocatalysis; thus, the excitation of electrons by photons at the ground state is the prerequisite. Periodically, the excitation stage and thus the photoexcitation of electrons at the ground state also occurs in most of the materials adsorbed on the surface of the semiconductors;<sup>97</sup> *e.g.*, the reaction occurring in dye-sensitized solar cells.<sup>42</sup> There are different pathways that are mainly experienced by the charge carriers. Many of the individual materials such as  $\text{TiO}_2$  are mostly used for water splitting, oxidation/reduction, (Fig. 5) in both suspension and electrode systems.

Significant research attention is centered on metal oxides and silicates due to their photocatalytic activities and their wide range of applications in photocatalysis.<sup>90</sup> Several semiconductors, such as  $\text{TiO}_2$ ,<sup>91</sup>  $\text{ZnO}$ ,<sup>81</sup>  $\text{Fe}_2\text{O}_3$ ,<sup>82</sup>  $\text{WO}_3$ ,<sup>75</sup>  $\text{SrTiO}_3$ ,<sup>76</sup>  $\text{NaTaO}_3$ ,<sup>77</sup>  $\text{CdS}$ ,<sup>78</sup>  $\text{Ag}_3\text{PO}_4$ ,<sup>75</sup>  $\text{BiPO}_4$ ,<sup>79</sup> and  $\text{g-C}_3\text{N}_4$ ,<sup>80</sup>  $\text{NiO}$ ,<sup>83</sup>  $\text{Cr}_2\text{O}_3$ ,<sup>84</sup>

$\text{Co}_3\text{O}_4$ ,<sup>85</sup>  $\text{Al}_2\text{O}_3$ ,<sup>89</sup> are known photocatalysts, with their use for effective photocatalytic activities being dependent on their band gap<sup>86–88</sup> (Fig. 6 and 7). The trapping experiments for holes and free radicals (ROS/RNS) are usually used to explain the photocatalytic schemes of photocatalysts such as  $\text{TiO}_2$ . Also, the trapping experiments of holes, hydroxyl radicals ( $\cdot\text{OH}$ ), and superoxide radicals ( $\cdot\text{O}_2^-$ ) have been reported by many studies in photocatalysis as the main oxidative species that are found in photocatalytic processes.

In instituting whether transformation or water splitting (Fig. 5) is really a photocatalytic activity, with direct activation of reactants and intermediates through visible light absorption, it is essential to establish that the photocatalyst absorbs the photons rather than the absorbents.<sup>92,93</sup>

Photoexcited charge carriers (Fig. 7) drive the conversion of water (Fig. 5) and carbon dioxide into  $\text{H}_2$ ,  $\text{CO}$ ,  $\text{CH}_4$ , and  $\text{CH}_3\text{OH}$  related oxygenates and hydrocarbons<sup>94–96</sup> during photocatalytic production.

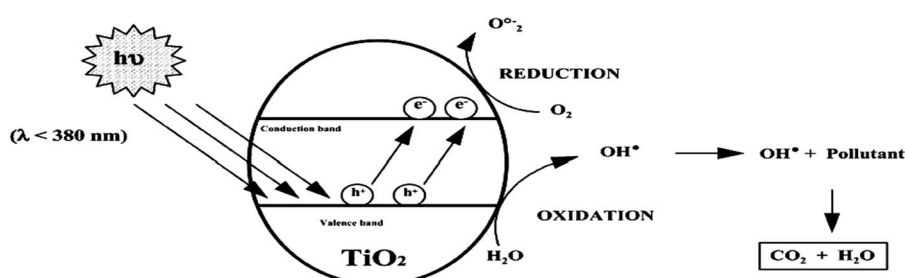


Fig. 7 Schematic picture of the principles of the photocatalytic degradation of non-porous  $\text{TiO}_2$  particles.



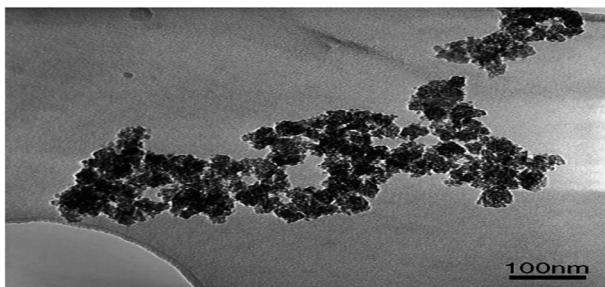


Fig. 8 TEM image of the synthesized  $\text{TiO}_2$ – $\text{SiO}_2$  catalyst. Reproduced with permission.<sup>66</sup> Copyright 2006, *Chemical Engineering and Processing*. Elsevier.

**2.1.1. Hybrid non-porous  $\text{TiO}_2$  photocatalysts.** The concentration of chemical compounds is determined by the rate of chemical reactions as described by Yu and coauthors.<sup>55</sup>  $\text{TiO}_2$  has low adsorption ability, specifically for nonporous compounds, which is as a result of its polar structure. The synthesis of  $\text{TiO}_2$  with adsorbents is an important factor in improving the adsorption properties of  $\text{TiO}_2$  particles; the adsorbents hold the compounds on the adsorbent support. Yu and coauthors<sup>45</sup> reported that an increase in the photoreaction rate comes about due to the formation of high environmental concentrations of the compounds around the nonporous  $\text{TiO}_2$  particle. Consequently, numerous schemes have been established to alter the properties of  $\text{TiO}_2$ , anticipating the lengthening of the lifespan of the photogenerated electron–hole pairs and a narrower band gap. To extend the optical absorption to the visible region and the lifetime of  $\text{TiO}_2$ , many successful studies by researchers in the field have centered on doping metal or non-metal elements into the  $\text{TiO}_2$  lattice to generate donors or acceptors in the band gap. However, there are substantial restrictions for this approach; the reduced incident photon to electron transformation efficiency in the UV light region and improved carrier recombination centers are the most challenging. Consequently, to heighten the useful application of  $\text{TiO}_2$ , it is important to decrease the recombination and then increase the visible light absorption.<sup>45</sup> Various adsorbents such as zeolite, alumina, silica, mordenite, ferrite, and activated carbon, have been used as the support for  $\text{TiO}_2$  and they have shown that the hybrid photocatalysts are effective in achieving high decomposition rates of propionaldehyde in the air. Ao and Lee<sup>46</sup> used activated carbon with  $\text{TiO}_2$  as the hybrid photocatalysts in their research and they made similar conclusions to those made by Yu and colleagues.<sup>55</sup> The photodegradation efficacy of  $\text{ZnO}$ , when synergized with activated carbon as the adsorbent, was found to be higher compared to  $\text{TiO}_2$ .

**2.1.2. Preparation of the  $\text{TiO}_2$  photocatalysts.** Preparation methods (Table 1) for nano-based composites include the hydrothermal technique and water-in-oil microemulsion<sup>29,49</sup>, the sol-gel method<sup>47</sup>, and vapor decomposition of titanium alkyl oxides or  $\text{TiCl}_4$  in oxygen.<sup>48</sup>

The  $\text{TiO}_2$  nanomaterial obtained is mostly based on the conditions used in its preparation. These include the following:

Table 1 Comparison of selected preparative techniques for nonporous  $\text{TiO}_2$  photocatalysts

Preparation methods	Comparison
(1) Hydrothermal	(1) Preparation of $\text{TiO}_2$ powder using this method usually uses liquid solutions as solvents to harvest the precursors. This usually occurs under increased temperature, $<250$ °C, <sup>50</sup> and high-pressure conditions (2) Crystalline products are often formed (Fig. 8), considering the nucleation and crystal development. These products have different compositions, structures, and morphologies. $\text{TiO}_2$ powders are obtained after critical washing and drying (3) $\text{NaOH}$ or ethanol and water frequently serve as the solvents. $\text{TiCl}_4$ and $\text{Ti}(\text{SO}_4)_2$ are also commonly used as precursors (4) The hydrothermal procedure is best used to improve crystallization on both the laboratory and commercial scales. The crystallization process <sup>51</sup> is influenced by features such as reaction time, reaction temperature, the medium, and type of precursor
(2) Water-in-oil microemulsion techniques	(1) In recent years, scientists in this field have shifted a lot of attention to monodisperse nanoparticle preparation using this technique <sup>49</sup> due to the following factors: (a) The water-in-oil microemulsion is thermodynamically stable <sup>52</sup> (b) It is also the optically isotropic dispersion of surfactant stabilized microdroplets of water in an external oil phase. <sup>52</sup> These extremely dispersed nanosized microdroplets are well-matched for particle synthesis. This is due to the ability to control the microenvironment, the site for chemical reactions
3. Coating methods	(1) Studies have revealed that active commercial $\text{TiO}_2$ powder possesses less photocatalytic activity than the $\text{TiO}_2$ film. <sup>53</sup> Photocatalytic activity is often influenced by coating the $\text{TiO}_2$ . <sup>53</sup> $\text{TiO}_2$ doped with elements such as C and N for doped $\text{TiO}_2$ synthesis is less expensive <sup>29</sup> (2) There are two main coating methods: (a) Directly sintering or dip-coating (sometimes called wash-coating) the catalyst powders <sup>54</sup> (b) Formation of the $\text{TiO}_2$ film on the support. This mostly uses the following preparative techniques: (i) Metal–organic CVD (MOCVD) <sup>19</sup> (ii) Chemical vapor deposition (CVD) (iii) Sol-gel <sup>40,55</sup> (iv) Spray coating

(1) Gas-phase method.

(2) Liquid-phase method.

**2.1.3. Point defects and standard specimens.** The idea of defects primarily lies in the solid state physics explanation of



lattice distortion. Lattice distortion is usually in the form of linear defects, point defects, three-dimensional valleys or hetero-impurities and two-dimensional flaws or interfaces. Fujishima and team found that point defects are well studied by scientists in the field and this delivers the principal understanding of the properties of lattice defects, consisting of magnetic, electrical, energetic, optical, and thermal characteristics in solids.<sup>2</sup> OTDs are commonly accepted as point defects. In photocatalytic reactions, the point trap model is best used to analyze oxygen vacancies and OTD-related clusters.<sup>43</sup> In the case of the synthesis process, lattice defects are certainly produced. These defects are thermal and preparation dependent.<sup>43</sup> During material doping, intrinsic point defects are often observed in the lattice. These observed intrinsic point defects exist as atomic impurities, vacancies and interstitials. Studies have shown that these defects are scattered on flat surfaces as observed by STM images. The scattered distribution of these defects is noted to be the main reason for most of the increased photocatalytic activities.

In contrast, the presence of the coordinate and disordered defects in diverse samples makes it barely possible to exactly compare the photocatalytic properties. Under ambient conditions at room temperature, distinct particles are uncommon.<sup>44</sup> To simplify the study on the molecular scale, much research has been devoted to the hypothesis pertaining to well-defined particles. Consequently, there is a strong call for the understanding of the nature of photocatalytic reactions regarding the preparation of comparable standard specimens.

## 2.2. Oxygen vacancy

Oxygen vacancy occurs when the number of oxygens anticipated in a particular compound is less than what it is supposed to have to make it a perfect crystal lattice. Annealing in a reducing atmosphere is a prerequisite for the removal of oxygen from a compound made up of oxygen. Extra oxygenation requires annealing in an oxidizing atmosphere ( $O_2$ ). Simply put, this involves hole doping (the removal of two electrons as a result of adding one oxygen atom from the parent atom), and electron doping (addition of two electrons due to the removal of one oxygen atom from the parent atom). Magnetic and transport properties are mostly determined by the final material's structure, which is also dependent on its total charge/spin state. This idea is expected to be true in nanomaterials or bulk materials; however, anomalous properties are seen in nanomaterials, due to the ability of these materials to exist in new or active electronic states or environments (Fig. 9).<sup>10</sup>

Considering spinel type ferrites, the exchange of cations in the tetrahedral and octahedral sites in these magnetic oxides are well known to induce vacancies or lattice defects. There is, therefore, the inversion of normal spinel structures due to the occupation of most divalent transitional metal ions. At this point, the superexchange mechanism is produced due to the relative positions of both octahedral and tetrahedral sites of the atoms. Interatomic distances, anions, cations and bond angles are extensively close. The hopping mechanism that has a give-and-take of an  $e^-$  to a half-filled shell is often determined by

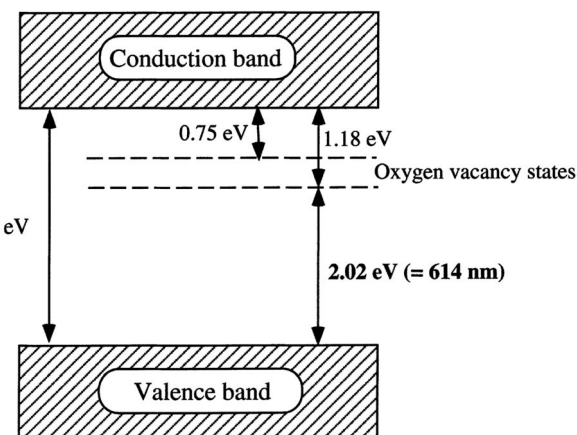


Fig. 9 A proposed band structure model for the anatase  $TiO_2$  with oxygen vacancies. Reproduced with permission.<sup>65</sup> Copyright 2000, *Journal of Molecular Catalysis A: Chemical*. Elsevier.

the oxygen atom in the structure. Antiferromagnetic coupling to the unpaired spin of oxygen, as described by the Pauli exclusion and Hund's rule, or contribution to the net magnetism occurs due to an outstanding exchange with the closest neighbor transition metal. Negative and positive oxygen vacancies are two main types of oxygen vacancy. The concentration is centered on the oxygen vacancy, one of the natural spots in oxides, due to the vital role it plays in the physical characteristics of materials.

**2.2.1. Oxygen vacancies and the photocatalytic activity of nonporous, and doped  $TiO_2$ .** Recently, a novel technique involving positron annihilation lifetime spectroscopy was used to characterize oxygen vacancy associated with hydrogenation modified  $TiO_2$ .<sup>2</sup> This research revealed that hydrogenated  $TiO_2$  contains some larger vacancy clusters, a massive amount of small neutral  $Ti^{3\pm}$  oxygen vacancies and a small number of voids of vacancies. The emergence of new Raman vibrations occurred as a result of these defects, which led to the atomic lattice high-resolution transmission electron microscopy (HRTEM) images.<sup>56</sup> The concentration of oxygen vacancies was measured by X-ray photoelectron spectroscopy (XPS) and this was found to be 3% in the  $TiO_2$  lattice. There was a remarkable increase in photocatalytic activity when the oxygen vacancies introduced by hydrogenation slowed the charge recombination; this was actually revealed by the photocurrent, photoluminescence (PL) spectroscopy, and degradation of methylene blue. Fujishima and research group adopted reduction in hydrogen atmosphere coupled with an impregnation process to prepare defective  $TiO_2$  with oxygen vacancies and Cu(II) nanocluster modification.<sup>2</sup> There was no improvement in the visible light from the  $TiO_2$  photocatalyst samples with optimum oxygen vacancy. Conversely, the photocatalytic enactments of  $TiO_2$  samples with a greater quantity of oxygen vacancies were sharply reduced; they even demonstrated much enriched visible light absorptions. Wang and group successfully used the hydrothermal method in their experiment to prepare platinum decorated  $TiO_{2-x}N_x$  via a facile one-pot route by using nanotubular titanic acid as a precursor.<sup>3</sup> They further evaluated the



Table 2 Comparison of the differences between doped  $\text{TiO}_{2x}\text{N}_x$  and  $\text{TiO}_2$  photocatalysts (Fig. 10)

Doped $\text{TiO}_{2x}\text{N}_x$ photocatalyst	$\text{TiO}_2$ photocatalyst
(a) Several nitrogen-doped $\text{TiO}_2$ samples (Fig. 10) <sup>7</sup> were found to photodegrade gaseous formaldehyde, <sup>8</sup> acetaldehyde, <sup>8,9</sup> acetone, <sup>10</sup> 2-propanol, <sup>11,12</sup> toluene, <sup>8,13</sup> and methylene blue	(a) Pure $\text{TiO}_2$ photocatalyst is usually less effective for photo depletion of methylene blue <sup>39</sup>
(b) $\text{TiO}_{2x}\text{N}_x$ (films and powders) has better photoactivity than $\text{TiO}_2$ under visible light irradiation <sup>29</sup> due to higher surface acidity (Fig. 10) <sup>29,30</sup>	(b) $\text{TiO}_2$ has less photocatalytic activity under visible light irradiation
(c) The active wavelength of $\text{TiO}_{2x}\text{N}_x$ , of less than 500 nm covers the main peak of the solar irradiation energy beyond the Earth's atmosphere (around 460 nm) <sup>9</sup>	(c) A similar active wavelength of 500 nm for $\text{TiO}_2$ does not cover the main peak of the solar irradiation energy beyond Earth's atmosphere <sup>9</sup>
(d) Introduction of $\text{ZrO}_2$ into $\text{TiO}_{2x}\text{N}_x$ exhibited higher porosity, higher specific surface area, and an enhanced thermal stability <sup>14</sup>	(d) This feature was absent in $\text{TiO}_2$
(e) Decreases the deactivation of the photocatalysts <sup>28</sup>	(e) Deactivation of the surface occurs very quickly

photocatalytic performance of  $\text{Pt}/\text{TiO}_{2-x}\text{N}_x$  for the visible-light-induced degradation of propylene in relation to the synergistic effect among single-electron-trapped oxygen vacancies and N plus Pt dopants. It was proposed that the synergistic effect among oxygen vacancies and dopants led to the enriched photocatalytic activity of the as-synthesized  $\text{Pt}/\text{TiO}_{2-x}\text{N}_x$ . The  $\text{TiO}_2$  photocatalyst spectral response to the visible light range is usually improved by impurity doping (Tables 2 and 3).<sup>32,37</sup> In 2015, experiments performed by Park and group showed that the maximum entropy method (MEM) analysis and X-ray diffraction (XRD) used in the analysis of the changes in the  $\text{V}_\text{O}$  concentration as a function of the Co-doping level from ZnO Rietveld refinement generated the same results but X-ray photoelectron spectroscopy (XPS) confirmed a different outcome.<sup>4</sup>

The Wendt group's experiment<sup>5</sup> on adsorption and desorption, where they used oxygen and water as probe molecules that were observed in STM images to bridge oxygen vacancies, and oxygen atoms on surface Ti atoms, reported the production of pure and reduced  $\text{TiO}_2$  surfaces. Their work further addressed the criteria to determine the cleanliness by STM imaging.<sup>5</sup> Yang and colleagues in their research in 2010 on Chinese housing energy and environment introduced a novel technique for the characterization of oxygen vacancy associates in mostly hydrogen modified  $\text{TiO}_2$  photocatalyst using positron

annihilation lifetime spectroscopy (PALS). They concluded that small neutral  $\text{Ti}^{3\pm}$  oxygen vacancies (large quantity), vacancy clusters (appreciably large in size), and voids of vacancies (just a few of them) were actually in hydrogenated  $\text{TiO}_2$ . In the research by Fujishima and coworkers,<sup>2</sup> there was a remarkable improvement in the photocatalytic activity of 2%  $\text{WO}_3$ – $\text{TiO}_2$  catalysts when an appropriate oxygen vacancy was employed by using  $\text{Fe}^{3+}$  as an electron acceptor under UV irradiation in 12 hours.

Researchers have found out that the controlled combustion of Ti metal in a natural gas flame can also be used to synthesize chemically modified n-type  $\text{TiO}_2$  by using carbon as a doping agent.<sup>8,15</sup> Inhibition of the charge recombination and trapping of the photoexcited electrons using these doped impurities (Table 3) also helps to increase the photocatalytic activity.<sup>33–36</sup> There are three methods for preparing the visible light responsive photocatalyst, namely, doping  $\text{TiO}_2$  with transition metal ions, doping nitrogen into  $\text{TiO}_2$  and utilizing sensitizing dyes.

Semiconductors such as sensitizing dye (higher band-gap), change the electron-transfer processes during the photocatalytic reaction as described by Vinodgopal and Kamat in the principle of photosensitization of a semiconductor.<sup>16</sup> Dye cation radicals<sup>17</sup> can be produced by injecting charge from the excited dye molecule into the conduction band of  $\text{TiO}_2$ .

Table 3 Typical metals for  $\text{TiO}_2$  photocatalyst doping

Metals	Properties	References
(1) Transition metal ions such as V, Cr, Mn, Fe, Co, Ni, or Cu	(1) Extend light absorption into the visible region (2) There is a considerable reduction in the photocatalytic activity in the UV region	27 and 41
(2) Presence of metals, such as $\text{Li}^+$ , $\text{Zn}^{2+}$ , $\text{Cd}^{2+}$ , $\text{Ce}^{3+}$ , $\text{Co}^{3+}$ , $\text{Cr}^{3+}$ , $\text{Fe}^{3+}$ , $\text{Al}^{3+}$ , $\text{Mn}^{2+}$ and Pt	(1) Considerably change the photocatalytic activity of $\text{TiO}_2$ (2) Sol-gel systems can be used to prepare the $\text{Mn}^+/\text{TiO}_2$ layers for phenol degradation	39 and 41
(3) The presence of $\text{Co}^{3+}$ , $\text{Cr}^{3+}$ , $\text{Ce}^{3+}$ , $\text{Mn}^{2+}$ , $\text{Al}^{3+}$ and $\text{Fe}^{3+}$ ion (5 mol% $\text{Mn}^+$ : $\text{Ti}^{4+}$ )	(1) Has an opposing influence on the photocatalytic activity of the $\text{TiO}_2$ photocatalyst (2) There is a decline in the photocatalytic activity of $\text{TiO}_2$ under UV irradiation (3) These metal ions act as recombination sites for the photogenerated charge carriers	41



**Table 4** Comparison of selected quantitative analysis tools for oxygen vacancy

Analysis tool	Comparison
(1) X-ray diffraction (XRD)	(1) X-ray diffraction (XRD) is a simple and useful tool for the analysis of oxygen vacancy because it reveals the crystal structure and the electron density distribution of periodic arrays of atoms (2) Analysis of X-ray diffraction data using Rietveld refinement has been attempted for the quantitative analysis of oxygen vacancies in terms of oxygen site occupancy (3) X-ray diffraction requires the use of neutrons or synchrotron X-rays
(2) Maximum entropy technique	(1) The maximum entropy method (MEM) is also a suitable tool for the analysis of oxygen because it uses the more precise Rietveld refinement that resolves summation-terminated errors and affords a better structural model (2) The maximum entropy technique presents insignificant modeling errors <i>via</i> the least-biased electronic reconstruction of X-ray diffraction patterns in real space

**2.2.2. Quantitative analyses of oxygen vacancies.** The quantitative analysis of oxygen vacancies has been successfully researched by many scientists in the field. Researchers have adopted the following oxygen vacancy quantitative analysis tools:

- (1) The maximum entropy method (MEM).
- (2) X-ray diffraction (XRD).

Most research efforts have also proposed a method for the analysis of oxygen vacancies using conventional XRD and MEM techniques (Table 4).

The efficiency of a particular photocatalyst depends strongly on the competence of electron–hole pair separation and the adsorption ability of gaseous oxygen vacancy compounds. Coupling TiO<sub>2</sub> catalysts<sup>18–20</sup> with other semiconductor oxides or depositing metals or doping TiO<sub>2</sub> photocatalysts with some other metal ions help to improve its photocatalytic activities. Studies have<sup>18</sup> established that the photoreactivity for both oxidation and reduction significantly improved when they doped with Fe<sup>3+</sup>, Mo<sup>5+</sup>, Ru<sup>3+</sup>, Os<sup>3+</sup>, Re<sup>5+</sup>, V<sup>4+</sup>, and Rh<sup>3+</sup> at 0.1–0.5%, but Co<sup>3+</sup> and Al<sup>3+</sup> doping decreased the photoreactivity.<sup>22</sup> When the active sites on the reaction surface<sup>21</sup> of a gas–solid photocatalyst is reduced, the activity also decreases.<sup>21</sup> It can be concluded that the activity of catalysts depends on their lifetime, which is potentially essential to the economic process.<sup>21</sup> Studies on toluene,<sup>23,24</sup> ethanol<sup>25</sup> and trichloroethylene, dimethyl sulfide, and trichloropropene<sup>22</sup> have found out that deactivation in these compounds is really uncommon. Sauer and Ollis<sup>26</sup> in their work stated that particle materials block pores on the photocatalysts' surfaces, hence, change the surfaces of these catalysts.<sup>27</sup> The chemical or physical adsorption of organic substrates on the TiO<sub>2</sub> matrix is improved when of lanthanide ions, for instance, La<sup>3+</sup>, Eu<sup>3+</sup>, Pr<sup>3+</sup>, Nd<sup>3+</sup>, and Sm<sup>3+</sup> amalgamated into the matrix<sup>19</sup>.

**2.2.3. The function of the TiO<sub>2</sub> oxygen vacancy in the energy structure.** The pristine energy structure of most

outstanding nanomaterials, such as TiO<sub>2</sub> is fabricated by the conduction band and valence band. It is noted that the development of the main active sites, mostly for visible light absorption and the band gap is supported by these energy levels. Lv and group stated that the function of oxygen vacancies as the visible light response sites is due to the defective TiO<sub>2</sub> surface during visible light irradiation.<sup>57</sup> The influence of the energy structure of the TiO<sub>2</sub> photocatalyst on the charge carrier migration and light absorption is very high (this happens when there is the removal of oxygen atoms; Ti<sup>3+</sup> is not involved and when there is the occurrence of oxygen vacancies). This calls for urgent, precise calculations of the defect state in TiO<sub>2</sub> energy structure.<sup>2</sup> Fujishima and group have reported that the defect states vary remarkably in the band gap. Recent work<sup>58</sup> reported lower energy (for all Fermi-level positions in the band gap) in oxygen vacancies. It has been proven that within the band gap of TiO<sub>2</sub>, the oxygen vacancy usually forms a mid-gap electronic state and, therefore, TiO<sub>2</sub> functions as the donor. This novel trend was supported by research performed by Eun Chang and colleagues.<sup>39</sup> These scientists further summarized energy levels of oxygen vacancies in TiO<sub>2</sub>. The paradox of the intensely localized small polarons and the delocalized free polarons failed to be explained vividly by isolating electronic bands in many experiments and this led to hybrid function, which has been a remarkable theory. In the electronic band, it was reported that there exist two types of hybrid functions:

- (a) Between the electrons and the conduction band in the presence of delocalized free electrons.
- (b) Between the electrons and the oxygen vacancies in the form of oxygen vacancy complexes and the ionized shallow-donor impurities.

Considering the theoretical viewpoint, the highest occupied molecular orbital and the lowest unoccupied molecular orbital often shifts due to the influence exerted by the defect states.<sup>59</sup> It was realized from experiment<sup>59</sup> that an occupied defect state of 0.7 eV below the bottom of the conduction band was decreased by the oxygen vacancy.<sup>7</sup> Research on the characterization analysis of anatase, rutile, and brookite showed that anatase and brookite were made up of oxygen vacancies, which remarkably improved the photocatalytic activity. In conclusion, it is presumed that the difference in the absorptions on the surfaces of the active sites and the reactants (CO<sub>2</sub>, H<sub>2</sub>O, CO<sub>3</sub><sup>2-</sup>, and CO) were due to oxygen vacancies.

**2.2.4. The influence of oxygen vacancies on charge transfer.** In situ-EPR is a versatile technique for monitoring the separation and transfer of photogenerated electrons in semiconductors based on oxides<sup>101,102</sup> or carbon nitrides<sup>98</sup> since electrons excited to the conduction band can be trapped at oxygen vacancies<sup>100</sup> and carbon defects.<sup>99</sup> The promotion from the highest occupied molecule orbitals to the lowest unoccupied molecule orbital with light irradiation causes the rapid movement of an excited single electron in response to the applied electric field; *i.e.*, the voltage supplied by a power source or difference in potential between the energy structure of TiO<sub>2</sub> and the redox potential of the adsorbed species (Fig. 10). Due to small lattice distortions in electron creation, the Franck–Condon factor is mostly small.<sup>60</sup> According to the Marcus–Hush



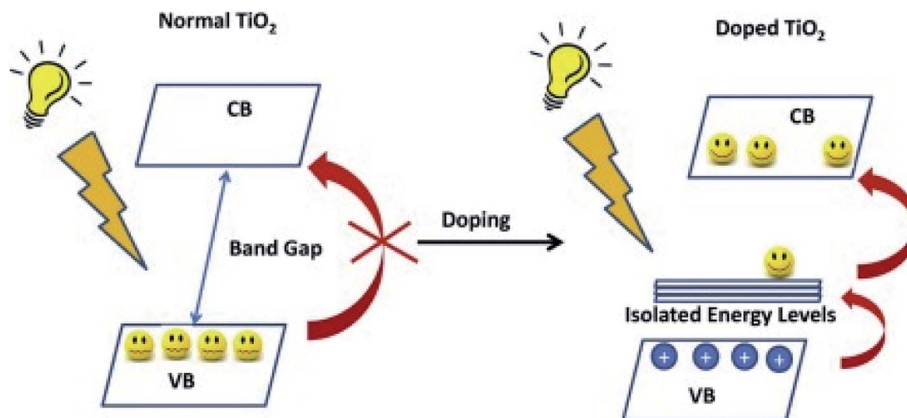


Fig. 10 Schematic diagram showing the activities of doped nonporous  $\text{TiO}_2$  and nonporous  $\text{TiO}_2$ .

electron transfer theory, the transfer of charge carriers is restricted by the disappearing reorganization of energy but it usually follows a band model and hopping model (Fig. 11).

Lattice distortion makes use of the original energy provided by an electron or a photon. The swiftly vanishing approach for the charge carriers<sup>7</sup> has been reported by many scientists as annihilation at the recombination center. Mitsuura and coworkers' studies<sup>43</sup> on semiconductors led to a proposal of three recombination mechanisms (Table 5).

#### 2.2.5. Applications of oxygen vacancies in photocatalysis.

The impact of oxygen vacancy in photocatalysis includes the following:

- (i) To alter the band energy structure of the pristine  $\text{TiO}_2$  as the defect states.
- (ii) To trap charge carriers in the migration pathways as the electron pool or recombination center.
- (iii) To power the adsorption of reactants (e.g.,  $\text{H}_2\text{O}$ ,  $\text{O}_2$ ,  $\text{CO}_2$ , and organic pollutants) as the active sites.<sup>61</sup>

### 3. Conclusion

This systematic review sums up the novel developments in the photocatalytic applications of  $\text{TiO}_2$ -based composite photocatalysts with oxygen vacancies in the areas of energy, wastewater treatment and environmental purification. Nonporous  $\text{TiO}_2$  has revealed its greatness as one of the best candidates in designing and engineering advanced composite photocatalysts. There is little doubt that the considerable progress in  $\text{TiO}_2$  nano-based composites will continue in the near future. More studies are necessary in order to make full use of the excellent properties resulting from the oxygen vacancy of the nonporous  $\text{TiO}_2$  photocatalysts.

Fig. 11 Diagram showing the charge transfer of the energy structure of  $\text{TiO}_2$ .

Table 5 Three recombination mechanisms, their properties and limitations

Recombination mechanism	Properties	Limitations	References
(1) Band-to-band recombination	(1) It occurs between the excited electron and the hole lying in the empty valence band (2) It is second order to the concentration of the charge carrier	(1) The production of available electrons and holes limits this reaction	61
(2) Trap-assisted recombination	(1) This mechanism transpires with the help of the "trap" state (2) It happens between the excited electrons and holes in the valence band	(1) Shockley-Read-Hall model (SRH model) confirmed that the concentration of charge carriers hinders this reaction or mechanism	
(3) Auger recombination	(1) This usually happens during the recombination process of the excited electron and hole (2) Releasing the energy to improve the energy of another electron or hole		20



## Conflicts of interest

The authors declare that they have no conflict of interest.

## Acknowledgements

This work was financially supported by grants from National Science Funds for Creative Research Groups of China (No. 51421006), Natural Science Foundation of China (51679063), the Key Program of National Natural Science Foundation of China (No. 41430751), the National Key Plan for Research and Development of China (2016YFC0502203), Fundamental Research Funds (No. 2016B43814), and PAPD. Buanya Beryl Adormaa and Williams Kweku Darkwah were the recipients of scholarship from the Nanjing Government and China Scholarship Council (CSC) respectively for the duration of this work.

## References

- 1 A. Fujishima and K. Honda, Electrochemical photolysis of water at a semiconductor electrode, *Nature*, 1972, **238**, 37–38.
- 2 A. Fujishima, *et al.*, Combination effect of activated carbon with  $TiO_2$  for the photodegradation of binary pollutants at typical indoor air level, *Sci. 80*, 2006, **4**, 2–4.
- 3 Y. Wang, *et al.*, Coiled-coil networking shapes cell molecular machinery, *Mol. Biol. Cell*, 2012, **23**, 3911–3922.
- 4 J. H. Park, *et al.*, Analysis of oxygen vacancy in Co-doped  $ZnO$  using the electron density distribution obtained using MEM, *Nanoscale Res. Lett.*, 2015, **10**, 186.
- 5 D. J. Wendt, *et al.*, Neutral Endopeptidase-Resistant C-Type Natriuretic Peptide Variant Represents a New Therapeutic Approach for Treatment of Fibroblast Growth Factor Receptor 3-Related Dwarfism, *J. Pharmacol. Exp. Ther.*, 2015, **353**, 132–149.
- 6 X. Yang, Y. Jiang, M. Yang and M. Shan, Energy and environment in Chinese rural housing: Current status and future perspective, *Front. Energy Power Eng. China*, 2010, **4**, 35–46.
- 7 Y. Liu and J. Brenan, Partitioning of platinum-group elements (PGE) and chalcogens (Se, Te, As, Sb, Bi) between monosulfide-solid solution (MSS), intermediate solid solution (ISS) and sulfide liquid at controlled  $fO_2-fS_2$  conditions, *Geochim. Cosmochim. Acta*, 2015, **159**, 139–161.
- 8 Y. Irokawa, *et al.*, Photodegradation of toluene over  $TiO_2-xNx$  under visible light irradiation, *Phys. Chem. Chem. Phys.*, 2006, **8**, 1116.
- 9 R. Asahi, T. Mikawa, T. Ohwaki, K. Aoki and Y. Taga, Visible Light Photocatalysis in Nitrogen-Doped Titanium Oxides, *Sci. 80*, 2001, **293**, 269–271.
- 10 T. Ihara, M. Miyoshi, Y. Iriyama, O. Matsumoto and S. Sugihara, Visible-light-active titanium oxide photocatalyst realized by an oxygen-deficient structure and by nitrogen doping, *Appl. Catal., B*, 2003, **42**, 403–409.
- 11 H. Irie, Y. Watanabe and K. Hashimoto, Nitrogen-Concentration Dependence on Photocatalytic Activity of  $TiO_2-xNx$  Powders, *J. Phys. Chem. B*, 2003, **107**, 5483–5486.
- 12 S. Miyauchi, *et al.*, Adaptation to left-right reversed vision rapidly activates ipsilateral visual cortex in humans, *J. Physiol.*, 2004, **98**, 207–219.
- 13 S. Wu, L. J. Mickley, D. J. Jacob, D. Rind and D. G. Streets, Effects of 2000–2050 changes in climate and emissions on global tropospheric ozone and the policy-relevant background surface ozone in the United States, *J. Geophys. Res.: Atmos.*, 2008, **113**, D18312.
- 14 P. Wang, The economics of foreign exchange and global finance, *Econ. Foreign Exch. Glob. Financ.*, 2005, DOI: 10.1007/s-540-28524-5.
- 15 R. Li, *et al.*, First report of the cyanotoxins cylindrospermopsin and deoxycylindrospermopsin from *Raphidiopsis curvata* (cyanobacteria) 1 A strain of *Raphidiopsis* (Cyanobacteria) isolated from a fish pond in Wuhan, P. R. China was examined for its taxonomy and pr, *J. Phycol.*, 2001, **1126**, 1121–1126.
- 16 K. Vinodgopal and P. V. Kamat, Enhanced Rates of Photocatalytic Degradation of an Azo Dye Using  $SnO_2/TiO_2$  Coupled Semiconductor Thin Films, *Environ. Sci. Technol.*, 1995, **29**, 841–845.
- 17 C. Nasr, *et al.*, Environmental photochemistry on semiconductor surfaces. Visible light induced degradation of a textile diazo dye, naphthol blue black, on  $TiO_2$  nanoparticles, *J. Phys. Chem.*, 1996, **100**, 8436–8442.
- 18 W. Choi, A. Termin and M. R. Hoffmann, The role of metal ion dopants in quantum-sized  $TiO_2$ : Correlation between photoreactivity and charge carrier recombination dynamics, *J. Phys. Chem.*, 1994, **98**, 13669–13679.
- 19 L. J. yi, M. W. hong, L. P. xiang and Z. J. cai, Detection of intermediates in the  $TiO_2$ -assisted photodegradation of Rhodamine B under visible light irradiation, *J. Environ. Sci.*, 2007, **19**, 892–896.
- 20 B. Zhang, X. Pan, C. H. Cannon, G. P. Cobb and T. A. Anderson, Conservation and divergence of plant microRNA genes, *Plant J.*, 2006, **46**, 243–259.
- 21 M. L. Sauer and D. F. Ollis, Photocatalyzed oxidation of ethanol and acetaldehyde in humidified air, *J. Catal.*, 1996, **158**, 570–582.
- 22 D. F. Ollis, Photocatalytic purification and remediation of contaminated air and water, *Comptes Rendus de l'Académie des Sciences - Series IIC - Chemistry*, 2000, **3**, 405–411.
- 23 M. A. Blanco, A. M. Pendás, E. Francisco, J. M. Recio and R. Franco, Thermodynamical properties of solids from microscopic theory: applications to  $MgF_2$  and  $Al_2O_3$ , *J. Mol. Struct.: THEOCHEM*, 1996, **368**, 245–255.
- 24 O. D'Hennezel, P. Pichat and D. F. Ollis, Benzene and toluene gas-phase photocatalytic degradation over  $H_2O$  and HCl pretreated  $TiO_2$ : By-products and mechanisms, *J. Photochem. Photobiol., A*, 1998, **118**, 197–204.
- 25 E. Piera, J. Ayllón, X. Doménech and J. Peral,  $TiO_2$  deactivation during gas-phase photocatalytic oxidation of ethanol, *Catal. Today*, 2002, **76**, 259–270.
- 26 M. L. Sauer and D. F. Ollis, Catalyst Deactivation in Gas – Solid Photocatalysis, *J. Catal.*, 1996, **217**, 215–217.



27 J. Zhao and X. Yang, Photocatalytic oxidation for indoor air purification: A literature review, *Building and Environment*, 2003, **38**, 645–654.

28 C. Belver, M. J. López-Muñoz, J. M. Coronado and J. Soria, Palladium enhanced resistance to deactivation of titanium dioxide during the photocatalytic oxidation of toluene vapors, *Appl. Catal., B*, 2003, **46**, 497–509.

29 X. Fu, L. a. Clark, Q. Yang and M. a. Anderson, Enhanced Photocatalytic Performance of Titania-Based Binary Metal Oxides:  $TiO_2/SiO_2$  and  $TiO_2/ZrO_2$ , *Environ. Sci. Technol.*, 1996, **30**, 647–653.

30 R. Méndez-Román and N. Cardona-Martínez, Relationship between the formation of surface species and catalyst deactivation during the gas-phase photocatalytic oxidation of toluene, *Catal. Today*, 1998, **40**, 353–365.

31 M. Chang and H. C. Chang, Development of a screening method for biogenic amine producing *Bacillus* spp., *Int. J. Food Microbiol.*, 2012, **153**, 269–274.

32 H. Kisch and W. Macyk, Visible-light photocatalysis by modified titania, *ChemPhysChem*, 2002, **3**, 399–400.

33 X. Chen, M. C. Schmidt, W. F. Goins and J. C. Glorioso, Two herpes simplex virus type 1 latency-active promoters differ in their contributions to latency-associated transcript expression during lytic and latent infections, *J. Virol.*, 1995, **69**, 7899–7908.

34 K. Nagaveni, M. S. Hegde, N. Ravishankar, G. N. Subbanna and G. Madras, Synthesis and Structure of Nanocrystalline  $TiO_2$  with Lower Band Gap Showing High Photocatalytic Activity, *Langmuir*, 2004, **20**, 2900–2907.

35 K. Nagaveni, G. Sivalingam, M. S. Hegde and G. Madras, Solar photocatalytic degradation of dyes: High activity of combustion synthesized nano  $TiO_2$ , *Appl. Catal., B*, 2004, **48**, 83–93.

36 L. T. Wong, K. W. Mui and P. S. Hui, A statistical model for characterizing common air pollutants in air-conditioned offices, *Atmos. Environ.*, 2006, **40**, 4246–4257.

37 D. T. Ho, A. J. Bardwell, S. Grewal, C. Iverson and L. Bardwell, Interacting JNK-docking sites in MKK7 promote binding and activation of JNK mitogen-activated protein kinases, *J. Biol. Chem.*, 2006, **281**, 13169–13179.

38 F. P. An, *et al.*, Observation of electron-antineutrino disappearance at Daya Bay, *Phys. Rev. Lett.*, 2012, **108**, 1–7.

39 E. C. Yang, K. M. Kim, J. Runess and S. M. Boo, Morphology and molecular phylogeny of *Psilotothallia dentata* (Ceramiaceae, Rhodophyta), *Algae*, 2004, **19**(4), 283–292.

40 W. T. Tseng, Z. Dörnyei and N. Schmitt, A new approach to assessing strategic learning: The case of self-regulation in vocabulary acquisition, *Appl. Linguist.*, 2006, **27**, 78–102.

41 P. V. Kamat and D. Meisel, Nanoparticles in advanced oxidation processes, *Curr. Opin. Colloid Interface Sci.*, 2002, **7**, 282–287.

42 T. Mitsuhasha, *et al.*, A Case of a Primary Radiation-Induced Malignant Peripheral Nerve Sheath Tumor in the Cauda Equina in a Patient with Neurofibromatosis, *Journal of Spine*, 2013, **2**, 2–4.

43 C. Di Valentin, L. Ferrighi and G. Fazio, Theoretical Studies of Oxygen Reactivity of Free-Standing and Supported Boron-Doped Graphene, *ChemSusChem*, 2016, **9**, 1061–1077.

44 C. Di Valentin, *et al.*, Adsorption of Water on Reconstructed Rutile  $TiO_2$  (011)-(2×1):  $TiO_2$  Double Bonds and Surface Reactivity, *J. Am. Chem. Soc.*, 2005, **127**, 9895–9903.

45 H. Yoneyama and T. Torimoto, Titanium dioxide/adsorbent hybrid photocatalysts for photodestruction of organic substances of dilute concentrations, *Catal. Today*, 2000, **58**, 133–140.

46 C. H. Ao and S. C. Lee, Combination effect of activated carbon with  $TiO_2$  for the photodegradation of binary pollutants at typical indoor air level, *J. Photochem. Photobiol., A*, 2004, **161**, 131–140.

47 H. Yu, Y. Ye, S. Zhao and G. Wang, A backprojection-filtration algorithm for nonstandard spiral cone-beam CT with an n-PI-window, *Phys. Med. Biol.*, 2005, **50**, 2099–2111.

48 L. Zeatoun and D. Feke, Characterization of  $TiO_2$  smoke prepared using gas-phase hydrolysis of  $TiCl_4$ , *Part. Part. Syst. Charact.*, 2006, **22**, 276–281.

49 P. Monnoyer, A. Fonseca and J. B. Nagy, Preparation of colloidal  $AgBr$  particles from microemulsions, *Colloids Surf., A*, 1995, **100**, 233–243.

50 S. Guo, *et al.*, Pulp and fiber characterization of wheat straw and eucaluptus pulps - A comparison, *BioResources*, 2009, **4**, 1006–1016.

51 J. Sun, L. Qiao, S. Sun and G. Wang, Photocatalytic degradation of Orange G on nitrogen-doped  $TiO_2$  catalysts under visible light and sunlight irradiation, *J. Hazard. Mater.*, 2008, **155**, 312–319.

52 Y. Qi, S. Bai and G. M. Heisler, Changes in ultraviolet-B and visible optical properties and absorbing pigment concentrations in pecan leaves during a growing season, *Agric. For. Meteorol.*, 2003, **120**, 229–240.

53 C. C. Huang, Z. Yang, K. H. Lee and H. T. Chang, Synthesis of highly fluorescent gold nanoparticles for sensing mercury(II), *Angew. Chem., Int. Ed.*, 2007, **46**, 6824–6828.

54 T. N. Obee and R. T. Brown,  $TiO_2$  Photocatalysis for Indoor Air Applications: Effects of Humidity and Trace Contaminant Levels on the Oxidation Rates of Formaldehyde, Toluene, and 1,3-Butadiene, *Environ. Sci. Technol.*, 1995, **29**, 1223–1231.

55 J. Yu, H. Elderfield and B. Hönnisch, B/Ca in planktonic foraminifera as a proxy for surface seawater pH, *Paleoceanography*, 2007, **22**, PA2202.

56 X. Feng, *et al.*, Significantly Enhanced Visible Light Photocatalytic Efficiency of Phosphorus doped  $TiO_2$  with surface oxygen vacancies for Ciprofloxacin Degradation: Synergistic Effect and Intermediates Analysis, *J. Hazard. Mater.*, 2018, DOI: 10.1016/j.hazmat.2018.03.013.

57 Y. Lv, Y. Zhu and Y. Zhu, Enhanced Photocatalytic Performance for the  $BiPO_4-x$  Nanorod Induced by Surface Oxygen Vacancy, *J. Phys. Chem. C*, 2013, **117**, 18520–18528.

58 L. Zou, Y. Luo, M. Hooper and E. Hu, Removal of VOCs by photocatalysis process using adsorption enhanced  $TiO_2-SiO_2$  catalyst, *Chem. Eng. Process.*, 2006, **45**, 959–964.



59 B. J. Morgan and G. W. Watson, Intrinsic n-type Defect Formation in TiO<sub>2</sub>: A Comparison of Rutile and Anatase from GGA+textit{U} Calculations, *J. Phys. Chem. C*, 2010, **114**, 2321–2328.

60 H. Kisch, *et al.*, Pseudotumor cerebri, *Neurol. Clin.*, 2004, **22**, 99–131.

61 J. Of, *et al.*, Oxygen Vacancy Structure Associated Photocatalytic Water Oxidation of BiOCl, *J. Phys. Chem. C*, 2013, **117**, 3601.

62 K. Zeitler, *Angew. Chem., Int. Ed.*, 2009, **48**, 9785.

63 N. M. Dimitrijevic, B. K. Vijayan, O. G. Poluektov, T. Rajh, K. A. Gray, H. He and P. Zapol, *J. Am. Chem. Soc.*, 2011, **133**, 3964.

64 M. R. Gholipour, C.-T. Dinh, F. Béland and T.-O. Do, Nanocomposite heterojunctions as sunlight-driven photocatalysts for hydrogen production from water splitting, *Nanoscale*, 2015, **7**, 8187–8208.

65 I. Nakamura, N. Negishi, S. Kutsuna, T. Ihara, S. Sugihara and K. Takeuchi, Role of oxygen vacancy in the plasma-treated TiO photocatalyst with visible light activity for NO removal, *J. Mol. Catal. A: Chem.*, 2000, **161**, 205–212.

66 L. Zou, Y. Luo, M. Hooper and E. Hu, Removal of VOCs by photocatalysis process using adsorption enhanced TiO<sub>2</sub>–SiO<sub>2</sub> catalyst, *Chem. Eng. Process.*, 2006, **45**, 959–964.

67 Y. Ma, X. Wang, Y. Jia, X. Chen, H. Han and C. Li, Titanium Dioxide-Based Nanomaterials for Photocatalytic Fuel Generations, *Chem. Rev.*, 2014, **114**, 9987–10043.

68 U. I. Gaya and A. H. Abdullah, Heterogeneous photocatalytic degradation of organic contaminants over titanium dioxide: A review of fundamentals, progress and problems, *J. Photochem. Photobiol. C*, 2008, **9**, 1–12.

69 J. Schneider, M. Matsuoka, M. Takeuchi, J. Zhang, Y. Horiuchi, M. Anpo and D. W. Bahnemann, Understanding TiO<sub>2</sub> Photocatalysis: Mechanisms and Materials, *Chem. Rev.*, 2014, **114**, 9919–9986.

70 S. N. Habisreutinger, L. Schmidt-Mende and J. K. Stolarczyk, Photocatalytic Reduction of CO<sub>2</sub> on TiO<sub>2</sub> and Other Semiconductors, *Angew. Chem., Int. Ed.*, 2013, **52**, 7372–7408.

71 R. Daghbir, P. Drogui and D. Robert, Modified TiO<sub>2</sub> for Environmental Photocatalytic Applications: A Review, *Ind. Eng. Chem. Res.*, 2013, **52**, 3581–3599.

72 K. Nakata and A. Fujishima, TiO<sub>2</sub> photocatalysis: Design and applications, *J. Photochem. Photobiol. C*, 2012, **13**, 169–189.

73 S. G. Kumar and L. G. Devi, Review on Modified TiO<sub>2</sub> Photocatalysis under UV/Visible Light: Selected Results and Related Mechanisms on Interfacial Charge Carrier Transfer Dynamics, *J. Phys. Chem. A*, 2011, **115**, 13211–13241.

74 S. J. A. Moniz, S. A. Shevlin, D. J. Martin, Z.-X. Guo and J. Tang, Visible-light driven heterojunction photocatalysts for water splitting—A critical review, *Energy Environ. Sci.*, 2015, **8**, 731–759.

75 W. Wang, B. Cheng, J. Yu, G. Liu and W. Fan, Visible-Light Photocatalytic Activity and Deactivation Mechanism of Ag<sub>3</sub>PO<sub>4</sub> Spherical Particles, *Chem.-Asian J.*, 2012, **7**, 1902–1908.

76 H. Kato and A. Kudo, Visible-Light-Response and Photocatalytic Activities of TiO<sub>2</sub> and SrTiO<sub>3</sub> Photocatalysts Codoped with Antimony and Chromium, *J. Phys. Chem. B*, 2002, **106**, 5029–5034.

77 H. Kato and A. Kudo, Water Splitting into H<sub>2</sub> and O<sub>2</sub> on Alkali Tantalate Photocatalysts ATaO<sub>3</sub> (A = Li, Na, and K), *J. Phys. Chem. B*, 2001, **105**, 4285–4292.

78 D. Jing and L. Guo, A Novel Method for the Preparation of a Highly Stable and Active CdS Photocatalyst with a Special Surface Nanostructure, *J. Phys. Chem. B*, 2006, **110**, 11139–11145.

79 C. Pan and Y. Zhu, New Type of BiPO<sub>4</sub> Oxy-Acid Salt Photocatalyst with High Photocatalytic Activity on Degradation of Dye, *Environ. Sci. Technol.*, 2010, **44**, 5570–5574.

80 X. Wang, K. Maeda, A. Thomas, K. Takanabe, G. Xin, J. M. Carlsson, K. Domen and M. Antonietti, A metal-free polymeric photocatalyst for hydrogen production from water under visible light, *Nat. Mater.*, 2009, **8**, 76–80.

81 Y. Lan, X. Li, G. Li and Y. Luo, Sol-gel method to prepare graphene/Fe<sub>2</sub>O<sub>3</sub> aerogel and its catalytic application for the thermal decomposition of ammonium perchlorate, *J. Nanopart. Res.*, 2015, **17**, 395.

82 M. Krumm, C. L. Pueyo and S. Polarz, Monolithic zinc oxide aerogels from organometallic sol-gel precursors, *Chem. Mater.*, 2010, **22**, 5129–5136.

83 J. G. Seo, M. H. Youn, Y. Bang and I. K. Song, Effect of Ni/Al atomic ratio of mesoporous Ni-Al<sub>2</sub>O<sub>3</sub> aerogel catalysts on their catalytic activity for hydrogen production by steam reforming of liquefied natural gas (LNG), *Int. J. Hydrogen Energy*, 2010, **35**, 12174–12181.

84 A. E. Gash, T. M. Tillotson, J. H. Satcher, Jr., L. W. Hrubesh and R. L. Simpson, New sol-gel synthetic route to transition and main-group metal oxide aerogels using inorganic salt precursors, *J. Non-Cryst. Solids*, 2001, **285**, 22–28.

85 T. Zeng, X. Zhang, S. Wang, H. Niu and Y. Cai, Spatial confinement of a Co<sub>3</sub>O<sub>4</sub> catalyst in hollow metal-organic frameworks as a nanoreactor for improved degradation of organic pollutants, *Environ. Sci. Technol.*, 2015, **49**, 2350–2357.

86 Z. Novak, P. Kotnik and Ž. Knez, Preparation of WO<sub>3</sub> aerogel catalysts using supercritical CO<sub>2</sub> drying, *J. Non-Cryst. Solids*, 2004, **350**, 308–313.

87 A. Cabañas, E. Enciso, M. C. Carbajo, M. J. Torralvo, C. Pando and J. A. R. Renuncio, Synthesis of SiO<sub>2</sub>-aerogel inverse opals in supercritical carbon dioxide, *Chem. Mater.*, 2005, **17**, 6137–6145.

88 R. Sui, A. Rizkalla and P. A. Charpentier, Experimental study on the morphology and porosity of TiO<sub>2</sub> aerogels synthesized in supercritical carbon dioxide, *Microporous Mesoporous Mater.*, 2011, **142**, 688–695.

89 M. B. Chowdhury, R. Sui, R. A. Lucky and P. A. Charpentier, One-pot procedure to synthesize high surface area alumina nanofibers using supercritical carbon dioxide, *Langmuir*, 2009, **26**, 2707–2713.



90 G. R. Patzke, Y. Zhou, R. Kontic and F. Conrad, Oxide nanomaterials: Synthetic developments, mechanistic studies, and technological innovations, *Angew. Chem., Int. Ed.*, 2011, **50**, 826–859.

91 E. Alonso, I. Montequi and M. Cocero, Effect of synthesis conditions on photocatalytic activity of TiO<sub>2</sub> powders synthesized in supercritical CO<sub>2</sub>, *J. Supercrit. Fluids*, 2009, **49**, 233–238.

92 M. Rochkind, S. Pasternak and Y. Paz, Using Dyes for Evaluating Photocatalytic Properties: A Critical Review. *Molecules*, 2015, **20**, 88–110.

93 N. Barbero and D. Vione, Why Dyes Should Not Be Used to Test the Photocatalytic Activity of Semiconductor Oxides, *Environ. Sci. Technol.*, 2016, **50**, 2130–2131.

94 S. Styring, Artificial photosynthesis for solar fuels, *Faraday Discuss.*, 2012, **155**, 357–376.

95 A. Listorti, J. Durrant and J. Barber, Solar to fuel, *Nat. Mater.*, 2009, **8**, 929–930.

96 D. Chen, X. Zhang and A. F. Lee, Synthetic strategies to nanostructured photocatalysts for CO<sub>2</sub> reduction to solar fuels and chemicals, *J. Mater. Chem. A*, 2015, **3**, 14487–14516.

97 Y. Nosaka and A. Y. Nosaka, Generation and Detection of Reactive Oxygen Species in Photocatalysis, *Chem. Rev.*, 2017, **117**, 11302–11336.

98 D. Hollmann, M. Karnahl, S. Tschierlei, K. Kailasam, M. Schneider, J. Radnik, K. Grabow, U. Bentrup, H. Junge, M. Beller, *et al.*, Structure-Activity Relationships in Bulk Polymeric and Sol-Gel-Derived Carbon Nitrides during Photocatalytic Hydrogen Production, *Chem. Mater.*, 2014, **26**, 1727–1733.

99 T. Li, L. Zhao, Y. He, J. Cai, M. Luo and J. Lin, Synthesis of g-C<sub>3</sub>N<sub>4</sub>/SmVO<sub>4</sub> composite photocatalyst with improved visible light photocatalytic activities in RhB degradation, *Appl. Catal., B*, 2013, **129**, 255–263.

100 J. B. Priebe, J. Radnik, A. J. J. Lennox, M.-M. Pohl, M. Karnahl, D. Hollmann, K. Grabow, U. Bentrup, H. Junge, M. Beller, *et al.*, Solar Hydrogen Production by Plasmonic Au-TiO<sub>2</sub> Catalysts: Impact of Synthesis Protocol and TiO<sub>2</sub> Phase on Charge Transfer Efficiency and H<sub>2</sub> Evolution Rates, *ACS Catal.*, 2015, **5**, 2137–2148.

101 K. Miyashita, S.-I. Kuroda, S. Tajima, K. Takehira, S. Tobita and H. Kubota, Photoluminescence study of electron-hole recombination dynamics in the vacuum-deposited SiO<sub>2</sub>/TiO<sub>2</sub> multilayer film with photo-catalytic activity, *Chem. Phys. Lett.*, 2003, **369**, 225–231.

102 A. Nashim, S. Martha and K. M. Parida, Heterojunction conception of n-La<sub>2</sub>Ti<sub>2</sub>O<sub>7</sub>/p-CuO in the limelight of photocatalytic formation of hydrogen under visible light, *RSC Adv.*, 2014, **4**, 14633–14643.

103 E. Karamian and S. Sharifnia, On the general mechanism of photocatalytic reduction of CO<sub>2</sub>, *J. CO<sub>2</sub> Util.*, 2016, **16**, 194–203.

104 J. L. White, M. F. Baruch, J. E. Pander, Y. Hu, I. C. Fortmeyer, J. E. Park, T. Zhang, K. Liao, J. Gu, Y. Yan, *et al.*, Light-Driven Heterogeneous Reduction of Carbon Dioxide: Photocatalysts and Photoelectrodes, *Chem. Rev.*, 2015, **115**, 12888–12935.

105 S. A. Lee, K. H. Choo, C. H. Lee, H. I. Lee, T. Hyeon, W. Choi and H. H. Kwon, Use of ultrafiltration membranes for the separation of TiO<sub>2</sub> photocatalysts in drinking water treatment, *Ind. Eng. Chem. Res.*, 2001, **40**, 1712–1719.

106 R. Molinari, L. Palmisano, E. Drioli and M. Schiavello, Studies on various reactor configurations for coupling photocatalysis and membrane processes in water purification, *J. Membr. Sci.*, 2002, **206**, 399–415.

107 W. Xi and S. Geissen, Separation of titanium dioxide from photocatalytically treated water by cross-flow microfiltration, *Water Res.*, 2001, **35**, 1256–1262.

108 D. B. Hamal, *et al.*, A multifunctional biocide/sporocide and photocatalyst based on titanium dioxide (TiO<sub>2</sub>) codoped with silver, carbon, and sulfur, *Langmuir*, 2010, **26**, 2805–2810.

109 B. Peng, *et al.*, General synthesis and optical properties of monodisperse multifunctional metal-ion-doped TiO<sub>2</sub> hollow particles, *J. Phys. Chem. C*, 2009, **113**, 20240–20245.

110 M. E. Kurtoglu, T. Longenbach, K. Sohlberg and Y. Gogotsi, Strong Coupling of Cr and N in Cr -N-doped TiO<sub>2</sub> and Its Effect on Photocatalytic Activity, *J. Phys. Chem. C*, 2011, **115**, 17392–17399.

111 F. Amano, M. Nakata, A. Yamamoto and T. Tanaka, Effect of Ti<sup>3+</sup>Ions and Conduction Band Electrons on Photocatalytic and Photoelectrochemical Activity of Rutile Titania for Water Oxidation, *J. Phys. Chem. C*, 2016, **120**, 6467–6474.

112 C. S. Chen, *et al.*, Effect of Ti<sup>3+</sup> on TiO<sub>2</sub>-supported Cu catalysts used for CO oxidation, *Langmuir*, 2012, **28**, 9996–10006.

113 H. Liu, *et al.*, The enhancement of TiO<sub>2</sub> photocatalytic activity by hydrogen thermal treatment, *Chemosphere*, 2003, **50**, 39–46.

114 I. Nakamura, S. Sugihara and K. Takeuchi, Mechanism for NO Photooxidation over the Oxygen-Deficient TiO<sub>2</sub> Powder under Visible Light Irradiation, *Chem. Lett.*, 2000, **29**, 1276–1277.

115 Z. K. Zhang, M. L. Bai, D. Z. Guo, S. M. Hou and G. M. Zhang, Plasma-electrolysis synthesis of TiO<sub>2</sub> nano/microspheres with optical absorption extended into the infra-red region, *Chem. Commun.*, 2011, **47**, 8439–8441.

